ME EN 5055, 27 April 2026

Parameters Affecting Performance of a Capacitive Microaccelerometer

Aidan Mulligan

***Abstract*— This paper investigates how key geometric design parameters affect the performance of a surface-micromachined capacitive accelerometer modeled in COMSOL Multiphysics. Parameter sweeps were conducted across three design domains: (a) spring geometry (width 2–4 µm; length 100–150 µm), (b) proof mass width (50–150 µm), and (c) electrode configuration (finger gap 1–2 µm, finger count 3-39, and finger overlap length 100-114 µm). Results confirm that changing spring stiffness (by changing spring length and width) is a highly effective measure for changing sensitivity and resonant frequency. Proof mass width is another parameter affecting sensitivity and resonant frequency, and can be changed by changing length or width of the proof mass. Electrode geometry is another area of interest for design. A narrower finger gap and higher finger count both increase capacitance and sensitivity nearly linearly, while finger overlap length shows decreased returns as it approaches maximum finger length. These findings provide a quantitative basis for optimizing MEMS accelerometer designs for target specifications.**

***Index Terms*—MEMS, capacitive microaccelerometer, spring design, proof mass, electrode configuration, sensitivity, resonant frequency, COMSOL.**

I. INTRODUCTION

MICROELECTROMECHANICAL systems (MEMS) accelerometers are indispensable for automotive safety, aerospace, wearable health monitoring, and consumer electronics. The first open-loop silicon accelerometer was demonstrated in 1979 by Roylance and Angell at Stanford University, an early example of a micromachined accelerometer [1]. Subsequent decades saw rapid development and commercialization of these devices [2].

Among the various transduction principles, capacitative accelerometers are common. Capacitive accelerometers exploit differential parallel-plate capacitance formed between comb fingers attached to a suspended proof mass and fixed stators. When an external acceleration deflects the proof mass, the resulting capacitance change (ΔC) can be used to determine rate of acceleration (g) based on device sensitivity. Device sensitivity (S_d) is determined by the following equation: $S_d = \frac{\Delta C}{g}$, and both sensitivity and resonant frequency depend on device design parameters [3]. This is why it is important to study the relationship between design parameters and capacitance, sensitivity, and resonant frequency.

This paper reports a systematic parameter-sweep study of a surface-micromachined accelerometer modeled in COMSOL Multiphysics, based on *Microsystem Design* by Senturia [4]. Three design domains are explored: (a) spring (flexure beam) geometry, (b) proof mass size, and (c) electrode (comb-finger) configuration. For each domain, simulation results are compared against theory, providing design insights applicable to device design.

II. MATERIALS AND METHODS

All simulations were performed in COMSOL Multiphysics using the given surface-micromachined accelerometer tutorial model (surface_micromachined_accelerometer.mph). The model solves the coupled electrostatics and structural-mechanics physics for a polysilicon comb-drive accelerometer. The baseline design corresponds to a sensing finger gap of 1 µm, 21 sensing fingers, a finger overlap length of 104 µm, a finger length of 114 µm, spring width of 2 µm, spring length of 280 µm, proof mass length of 448 µm, and proof mass width of 100 µm. Sensitivity was quantified as the raw sense voltage (es.fp1.V0 × 1000, in units of mV), evaluated under an applied acceleration of 50 g. Previous studies have evaluated sensitivity in terms of mV/g, so relating sensitivity to mV at a constant g of 50 will give interpretable results [3] [5]. Capacitance was recorded as the Maxwell capacitance es.C11. Resonant frequencies were obtained from a separate eigenfrequency study, which was run at eigenfrequency mode numbers of 1 to 6. The most reasonable eigenfrequency results were chosen for the paper.

A. Spring Design Effects

Spring width was parametrically swept over {2.0, 2.5, 3.0, 3.5, 4.0} µm. A step of 0.25 µm produced a solver failure at 3.25 µm, which is why a larger step of 0.5 µm was adopted. Spring length was swept over {100, 110, 121, 130, 140, 150} µm; the 120 µm case failed to converge in the solver, which is why 121 µm was substituted. For both width and length, both a stationary (sensitivity) and an eigenfrequency study were run. All other parameters were held at baseline values.

B. Proof Mass Effects

Proof mass width was parametrically swept over {50, 55, 60, …, 150} µm (5 µm steps), with all other parameters at baseline. Sensitivity and resonant frequency were measured by conducting both a stationary study and an eigenfrequency study. The baseline width of 100 µm would be compared against all other values in the parametric sweep.

C. Electrode Configuration

Three electrode (sensing finger) studies were performed. In each study, sensitivity (mV) and capacitance (es.C11) were recorded while control parameters remained at baseline.

First, finger gap was swept over {1.0, 1.2, 1.4, 1.6, 1.8, 2.0} µm; the 1.3 µm case exceeded COMSOL's degree-of-freedom limit and was omitted.

Second, sensing finger count was swept over {3, 6, 9, 12, 18, 21, 24, 27, 30, 33, 36, 39}; the case of 15 sensing fingers failed to solve and was excluded. Proof mass length was linearly changed to accommodate the number of fingers, based on the following equation: $L_{PM} = 448\mu m + 3 \times (n_f - 21) \times (W_f + g_f)$, where n_f is sensing finger count, W_f is finger width, and g_f is finger gap. Because the proof mass $m \propto L_{PM} W_{PM}$, the proof mass width was set to be equal to $W_{PM} = \frac{44800}{L_{PM}}$, which makes the proof mass constant at any the length.

Third, finger overlap length was swept over {100, 102, 104, 106, …, 114} µm; values below 100 µm caused solver failures and could not be tested.

III. Results

A. Spring Design Effects

The results for spring design are summarized below. We investigated how spring length and width affect device sensitivity and resonant frequency.

First, the relationship between sensitivity and spring width was investigated. As seen in Fig. 1, the sensor voltage (a measure of sensitivity) decreases at a fast rate with respect to spring width, and the function seems to follow a power law.

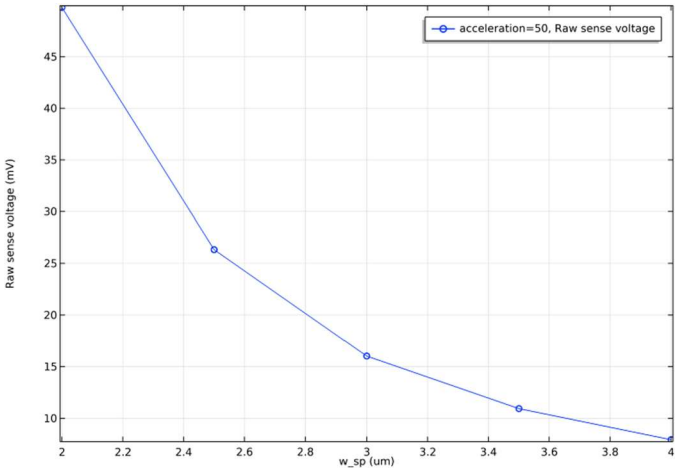

Fig. 1. Sensitivity as a function of spring width. Note that sensitivity decreases with spring width at a declining rate.

Next, the relationship between resonant frequency and spring width was investigated. As seen in Fig. 2, the resonant frequency increases with respect to spring width. This is true for all three eigenfrequencies on the chart.

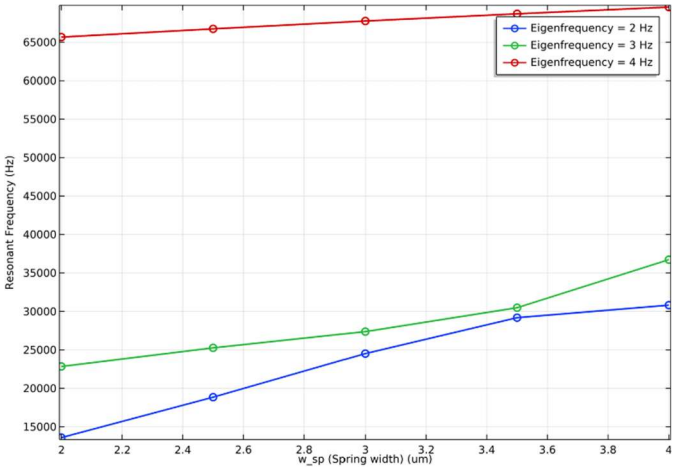

Fig. 2. Resonant frequency as a function of spring width for different eigenfrequencies. Resonant frequency increases with increased spring width.

When the relationship between sensitivity and spring length was investigated, the sensitivity was found to increase with respect to spring length. As seen in Fig. 3, sensitivity growth increases with increased length.

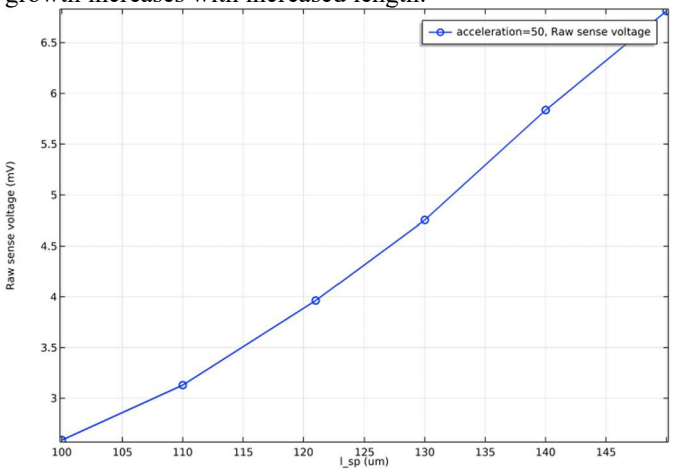

Fig. 3. Sensitivity as a function of spring length. Note that the chart curves upwards, and sensitivity increases with spring length.

Resonant frequency decreases as spring length increases, which can be seen in Fig. 4. The rate of decrease gets smaller as spring length increases, which is true for eigenfrequencies from a mode number of 2 to 4.

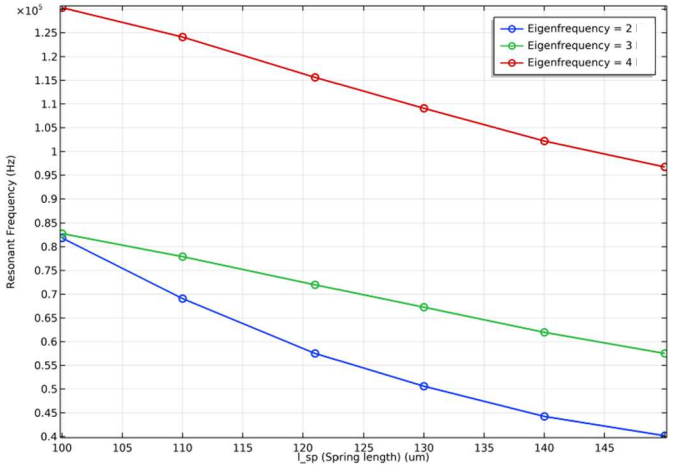

Fig. 4. Resonant frequency as a function of spring length for different eigenfrequencies. Resonant frequency decreases as spring length increases.

B. Proof Mass Effects

The results for proof mass width are summarized below. We investigated how proof mass width affects device sensitivity and resonant frequency.

When the relationship between proof mass width and sensitivity was investigated, the sensitivity was found to increase at a roughly linear rate with respect to proof mass width (Fig. 5).

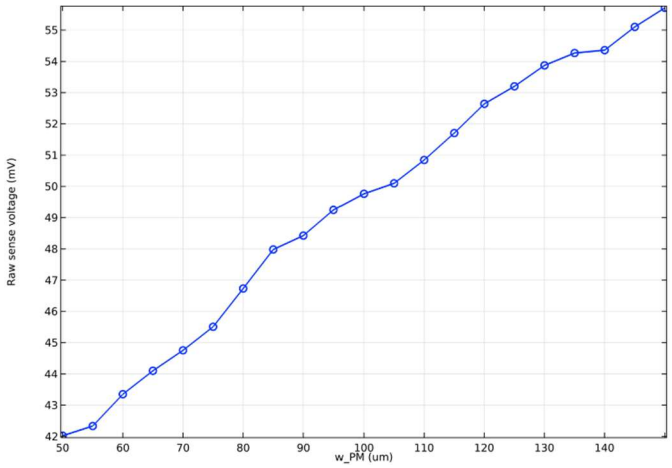

Fig. 5. Sensitivity as a function of proof mass width. Note that sensitivity increases mostly linearly as spring width increases.

Fig. 6 shows that resonant frequency decreases with respect to proof mass width. This is true for eigenfrequencies of a mode number from 1 to 3.

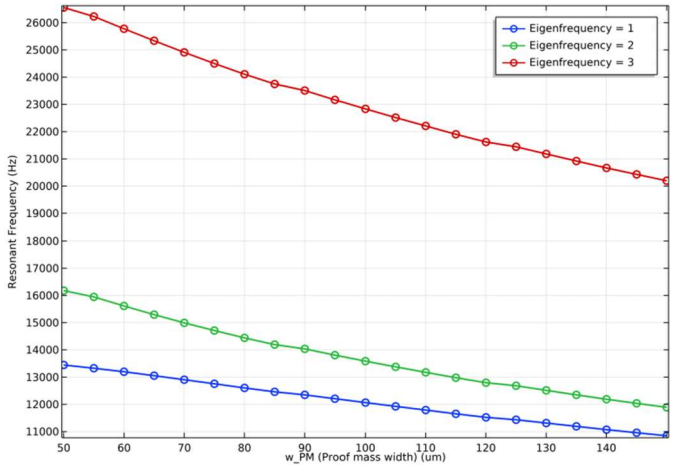

Fig. 6. Resonant frequency as a function of proof mass width for different eigenfrequencies. Note that resonant frequency decreases as proof mass width increases.

C. Electrode Configuration

The results for electrode configuration are summarized below. We investigated how finger gap, sensing finger count, and finger overlap length affect device sensitivity and capacitance.

The relationship between capacitance and finger overlap length shows a trend where capacitance increases as finger gap is decreased. However, the trend changes between 1.2 and 1.4 µm, where the capacitance drops dramatically as finger gap is decreased (Fig. 7). The decrease likely occurs at around 1.3 um, a value which could not be simulated by COMSOL because there were too many degrees of freedom.

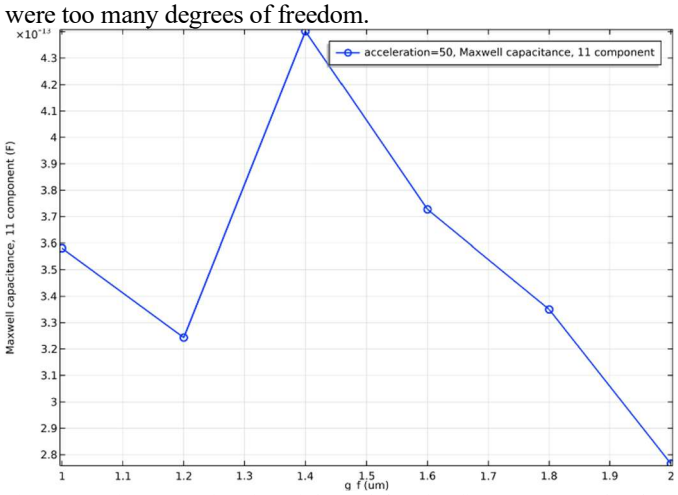

Fig. 7. Capacitance as a function of electrode/sensing finger gap. Note that there is a linear relation between for all finger gaps of 1.4 um or larger.

Sensitivity was found to be low for all finger overlap lengths tested except for 1.4 µm, which can be seen in Fig. 8.

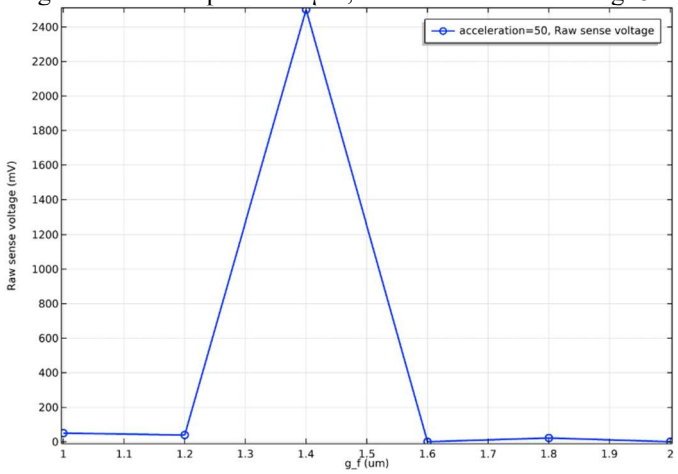

Fig. 8. Sensitivity as a function of electrode/sensing finger gap. Notice that sensitivity is low for all tested gaps except 1.4 um.

A highly linear trend was observed between the number of sensing fingers and capacitance (Fig. 9). COMSOL could not simulate 15 sensing fingers, so that point was not measured.

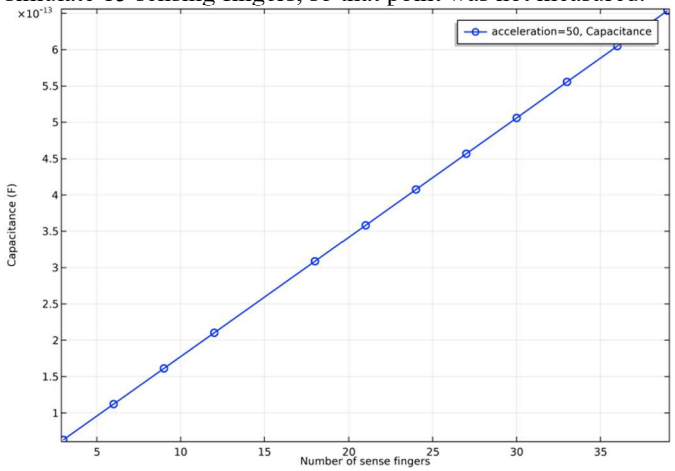

Fig. 9. Capacitance as a function of sensing finger count. Notice the highly linear trend.

Sensitivity was found to increase with respect to an increased number of sensing fingers (Fig. 10). The trend is mostly linear, except for a small decrease at around 33 sensing fingers.

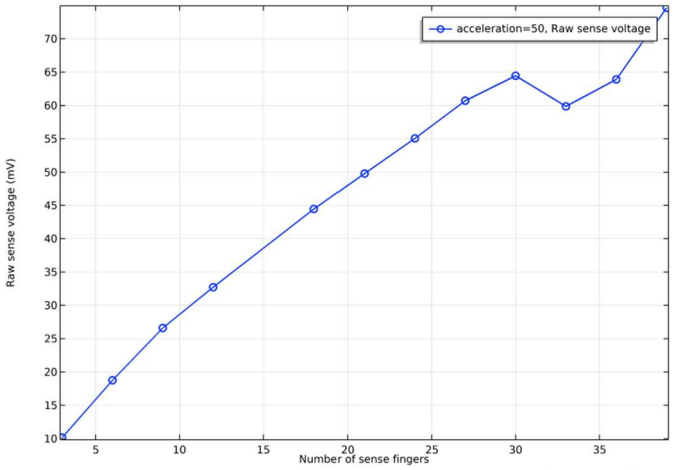

Fig. 10. Sensitivity as a function of sensing finger count. Note the generally linear trend.

As the sensing finger overlap length is increased from 100 to 114 µm, the capacitance tends to increase (Fig. 11). This is true for all values, except an overlap length of 112 µm.

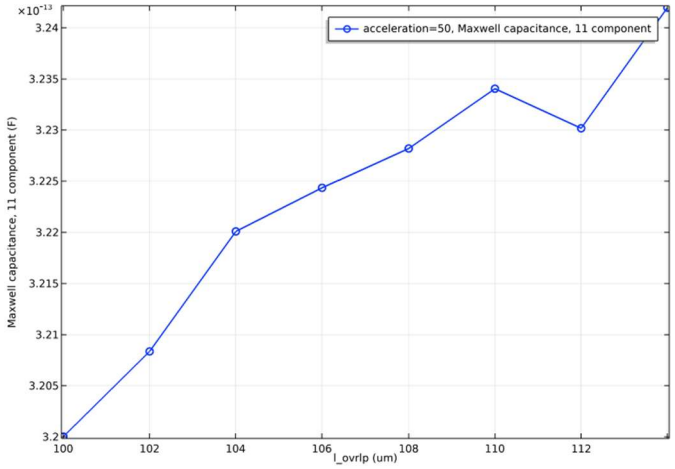

Fig. 11. Capacitance as a function of sensing finger overlap length. Note that capacitance increases with respect to overlap length.

Sensor sensitivity remains generally constant for most finger overlap lengths, as seen in Fig. 12. However, As finger overlap length is increased from 112 µm to 114 µm, sensitivity drops suddenly drops to 0. 114 µm is the finger length.

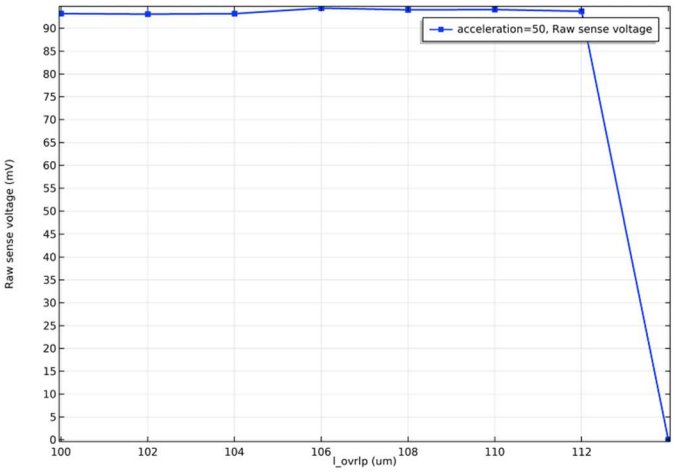

Fig. 12. Sensitivity as a function of sensing finger overlap length. Note the sudden drop as overlap length increases from 112 to 114 µm.

IV. Discussion

A. Spring Design Effects

Our simulation results are summarized again in Table 1 below. The table shows the effect of increasing width/length of the spring on sensitivity and resonant frequency. The sensitivity effect was much greater than the resonant frequency effect for all changes. It was found that increasing width decreases sensitivity and increases resonant frequency, while increasing length increases sensitivity and decreases resonant frequency.

Additionally, we know that $k \propto Et\frac{w^3}{L^3}$ for a spring. Thus, the effect of parameter changes on the spring constant has been included in the table.

TABLE I
SPRING LENGTH/WIDTH EFFECTS

Design change	Effect on k	Effect on sensitivity	Effect on resonant f
Increase Width	Strong increase	Strong decrease	Increase
Increase Length	Strong decrease	Strong increase	Decrease

The above results are expected and follow sensitivity trends seen in previous studies. In 2009, Tosserams et al. showed that the relationship $S_a \propto \frac{m}{k}$ is true for sensitivity [3]. Substituting the spring constant equation gives $S_a \propto m\frac{L^3}{W^3} \propto \frac{L^3}{W^3}$. This equation explains why our simulation shows such a strong decrease in sensitivity when width is increased, and such a strong decrease in sensitivity when length is increased.

The COMSOL results also confirm trends in resonant frequency from previous studies. According to Tosserams et al. the equation $f_n \propto \sqrt{k/m}$ gives the resonance frequency [3]. Substituting for k gives $f_n \propto \sqrt{\frac{w^3}{L^3 m}} \propto \sqrt{\frac{w^3}{L^3}}$, which makes sense in context of the COMSOL results. The effect of changing width and length on resonant frequency is the opposite of the effect on sensitivity. Additionally, the effect is less strong because of the square root operation.

Our COMSOL simulation data supported the conclusions of previous studies regarding the relationships between spring length/width, and sensitivity/resonant frequency. Notably, the effect is larger for sensitivity than resonant frequency. This means that changing spring length and width is a very powerful tool for changing sensor sensitivity. It is also a powerful tool for changing frequency, but to a lesser degree. Engineers may use this to design sensors with very high or low sensitivities.

B. Proof Mass Effects

In our results, we found that there is a roughly linear relationship between sensitivity and proof mass width. This is an expected result. According to Tian et al., we know that $m = \rho t L_m W_m$ gives the proof mass [2]. Additionally, Tosserams et al. show that the relationship $S_a \propto \frac{m}{k}$ is true for sensitivity [3]. Substitution results in the equation: $S_a \propto \rho t L_m W_m / k$, which means that $S_a \propto W_m$. According to that proportionality, there is an expected linear relationship between sensitivity and proof mass width, and our COMSOL simulation results support this conclusion.

Our results also showed an inverse relationship between resonance frequency and proof mass width at the tested eigenfrequencies. This is an expected result, as according to Tosserams et al. the equation $f_n \propto \sqrt{k/m}$ gives the resonance frequency [3]. Substitution results in the following equation: $f_n \propto \sqrt{k/\rho t L_m W_m}$, which means that $f_n \propto \sqrt{W^{-1}}$. The COMSOL data supports a similar relationship.

Our COMSOL simulation data supported the conclusion of previous studies, that there is a linear relationship between sensitivity and proof mass width, and an inverse relationship between resonant frequency and proof mass width. This makes proof mass width a useful measure to increase sensitivity and decrease resonance frequency in a design. Additionally, it should be noted that similar results occur from changing proof length rather than width. Because the proof mass bends (which may result in friction), engineers should be careful to balance the width and length of the proof mass to prevent bending.

C. Electrode Configuration

Our simulation results for electrode (sensing finger) gap showed that capacitance change increases linearly as finger gap is decreased, up until approximately 1.4 μm. At gaps shorter than 1.4 μm, there is a sudden decrease in capacitance change of the sensor. This suggests that there is a nonlinearity risk. Smaller gaps result in higher capacitance, as would be expected from a parallel plate capacitor. However, intermolecular forces make the fingers stick to each other at sufficiently small gaps, resulting in a decrease in capacitance change.

Simulation results also found that sensitivity was low for all overlap lengths tested except for 1.4 μm. This result is interesting, as it suggests a method of greatly increasing sensor sensitivity. The electrode gap of 1.4 μm was the smallest gap before our capacitance encountered a nonlinearity risk. Thus, sensitivity is highest at the smallest gap size before nonlinearity. Engineers can increase sensitivity by decreasing the gap size as much as possible, before sticking occurs. However, the gap size must not be too small, as that would result in nonlinearity at high accelerations. Thus, we can sacrifice sensor bandwidth for increased sensitivity (and vice-versa).

Simulation results revealed an extremely linear trend between capacitance and number of sensing fingers. Additionally, it was found that sensitivity increases at a roughly linear pace when the number of sensing fingers increases. These results demonstrate that sensing finger count is an extremely reliable tool to modify device capacitance and sensitivity in a predictable fashion. Although the change is not extreme, it is predictable enough to make finger count an effective design parameter.

Sensing finger overlap is another parameter that was studied in COMSOL simulations. These simulations discovered that capacitance tended to increase as the overlap was increased from 100 μm to the maximum finger length of 114 μm. On the other hand, sensitivity was mostly constant along the range, before a sudden decrease in sensitivity at the maximum finger length of 114 μm. These results demonstrate that a higher sensing finger overlap is beneficial, but that we can not have an overlap that is the same size as the maximum finger size. If the overlap and finger size are the same, then friction will decrease sensor sensitivity. Thus, it is beneficial to have a higher sensor overlap, but not high enough for there to be friction between fingers.

V. Conclusion

This report has quantified the sensitivity of a MEMS capacitive accelerometer using COMSOL Multiphysics simulations by changing parameters of the spring, proof mass, and electrode. Spring geometry governs the spring constant (k), and by changing spring length/width we can attain a desired sensitivity and resonant frequency for a sensor. Proof mass size provides a secondary measure of control over sensitivity and resonance frequency, although it has a less significant effect than the spring. Finally, electrode geometry (finger count, gap, and overlap) allows us to change the capacitance and sensitivity in a highly predictable way without making major changes to the mechanical design of the spring and proof mass system.

Together, these findings provide actionable design guidelines: to increase sensitivity, lower-stiffness springs or a heavier proof mass are preferred. Additionally, minor changes can be made by modifying the electrode system. Future work could include extending the study to out-of-plane modes, incorporating squeeze-film air damping in the coupled simulation, and exploring the benefit of other structural materials like SiC [2] [6].

Large Language Model (LLM) Usage Statement

This report was prepared with assistance from Claude Sonnet 4.6 (Anthropic) and Microsoft Copilot (April 2026 version). The LLMs were primarily used for drafting parts of the abstract, introduction, methods, and conclusion (approximately 30% of the final content), and for improving clarity. All COMSOL simulations and figures were designed and interpreted entirely by the author. All LLM outputs were thoroughly reviewed, edited, and fact-checked for the report's content and accuracy.

References

[1] L. M. Roylance and J. B. Angell, "A Batch-Fabricated Silicon Accelerometer," *IEEE Transactions on Electron Devices,* vol. 26, no. 12, pp. 1911-1917, December 1979.

[2] X. Tian, W. Sheng, Z. Guo, X. Weiwei and R. Tang, "Modeling and Analysis of a SiC Microstructure-Based Capacitive Micro-Accelerometer," *Materials,* vol. 14, no. 20, p. 1 to 18, 19 October 2021.

[3] S. Tosserams, L. F. P. Etman and J. E. Rooda, "A micro-accelerometer MDO benchmark problem," *Structural and Multidisciplinary Optimization,* vol. 41, pp. 255-275, 2009 September 2009.

[4] S. D. Senturia, Microsystem Design, 1, Ed., New York, New York: Springer, 2001.

[5] C.-K. Wang, K.-A. Wen and C.-S. Chen, "A monolithic CMOS MEMS accelerometer with chopper correlated double sampling readout circuit," in *2011 IEEE International Symposium of Circuits and Systems (ISCAS)*, Rio de Janiero, 2011.

[6] X. Tian, S. Wei, F. Tian, Y. Lu and L. Wang, "Simulation study on squeeze film air damping," *Micro & Nano Letters,* vol. 15, no. 9, pp. 576-581, 1 August 2020.